

Supporting information

External Fields Engineered Tunable Chern Number and Valley-Polarized Quantum Anomalous Hall Effect in $\text{Ti}_3\text{S}_3\text{Te}_2$ Monolayer

Xiaokang Xu,^{1#} Jinlian Lu,^{2#} Huijie Lian,³ Ying Han,¹ Yongjun Liu,¹ Xueke Yu,¹ Ailei He,^{1*} Xiaojing Yao,^{3*} Xiuyun Zhang^{1*}

¹ College of Physics Science and Technology, Yangzhou University, Yangzhou 225002, China.

² Department of Physics, Yancheng Institute of Technology, Yancheng, Jiangsu 224051, China.

³ College of Physics and Hebei Advanced Thin Films Laboratory, Hebei Normal University, Shijiazhuang 050024, China.

Email: A. L. He: heailei@yzu.edu.cn; X. J. Yao: xjyao@hebtu.edu.cn; X. Y. Zhang: xyzhang@yzu.edu.cn

The matrix elements of each term can be obtained by equation (1) and Fig.1(a). The equation (1) is Hamiltonian of real space.

The basis vector of TB model is $\mathbf{R}_1=[1,0,0]$; $\mathbf{R}_2=[-0.5, \sqrt{3}/2, 0]$, $\mathbf{R}_3=[0.0,0.0,1.0]$.

The position vector of each site is as follows:

$\mathbf{A}_1 : \mathbf{r}_0=[0.4,0.0,0.0]$; $\mathbf{A}_2 : \mathbf{r}_1=[0.0,0.4,0.0]$; $\mathbf{A}_3 : \mathbf{r}_2=[0.6,0.6,0.0]$

$\mathbf{B}_1 : \mathbf{r}_3=[0.333,0.666,-0.15]$; $\mathbf{B}_2 : \mathbf{r}_4=[0.666,0.333,0.15]$; $\mathbf{B}_3 : \mathbf{r}_5=[0.0,0.0,0.0]$

$\mathbf{C}_1 : \mathbf{r}_6=[0.333,0.666,0.15]$; $\mathbf{C}_2 : \mathbf{r}_7=[0.666,0.333,-0.15]$.

Here we provide each matrix element of the matrix in Table R1, in which $r_{ij}=r_j-r_i$. We only provided half of the matrix elements because the other half can be obtained through complex conjugation operations.

Table R1. Matrix elements of the Hamiltonian obtained by equation (1) and Fig.1(a).

| | 0 | 1 | 2 | 3 | 4 | 5 | 6 | 7 |
|---|--|---|-------------------------------|---------------------|---|---|---|---|
| 0 | -0.55 | | | | | | | |
| 1 | $t_1 e^{-i\phi} e^{ik(r_{01} - R_2)}$ + $t_1 e^{-i\phi} e^{ik(r_{01} + R_1)}$ $+ t_2 e^{ikr_{01}}$ | -0.55 | | | | | | |
| 2 | $t_1 e^{i\phi} e^{ik(r_{02} - R_2)}$ $+ t_1 e^{i\phi} e^{ikr_{02}} +$ $t_2 e^{ik(r_{02} - R_1 - R_2)}$ | $t_1 e^{-i\phi} e^{ikr_{12}} +$ $t_1 e^{-i\phi} e^{ik(r_{12} - R_1)}$ + $t_2 e^{ik(r_{12} - R_1 - R_2)}$ | -0.55 | | | | | |
| 3 | $t_B e^{ik(r_{03} - R_2)}$ | $t_B e^{ikr_{13}}$ | $t_B e^{ikr_{23}}$ | 0 | | | | |
| 4 | $t_B e^{ikr_{04}}$ | $t_B e^{ik(r_{14} - R_1)}$ | $t_B e^{ikr_{24}}$ | 0 | 0 | | | |
| 5 | $t_{B'} e^{ikr_{05}}$ | $t_{B'} e^{ikr_{15}}$ | $t_{B'} e^{ik(r_{25} - R_2)}$ | 0 | 0 | 0 | | |
| 6 | $t_C e^{ik(r_{06} - R_2)}$ | $t_C e^{ikr_{16}}$ | $t_C e^{ikr_{26}}$ | 0 | $t' e^{ikr_{46}} +$ $t' e^{ik(r_{46} - R_2)}$ + $t' e^{ik(r_{46} + R_1)}$ | 0 | 0 | |
| 7 | $t_C e^{ikr_{07}}$ | $t_C e^{ik(r_{17} - R_1)}$ | $t_C e^{ikr_{27}}$ | $t' e^{ikr_{37}} +$ | 0 | 0 | 0 | 0 |

| | | | | | | | |
|--|--|--|--|---------------------------|--|--|--|
| | | | | $t' e^{ik(r_{37} + R_2)}$ | | | |
| | | | | + | | | |
| | | | | $t' e^{ik(r_{37} - R_1)}$ | | | |

The phonon spectrum in Fig. S1(a) reveals a tiny imaginary-frequency mode in the Brillouin zone, indicating the dynamical stability of the monolayer $\text{Ti}_3\text{S}_3\text{Te}_2$. The formation energy (E_f) of monolayer $\text{Ti}_3\text{S}_3\text{Te}_2$ was expressed as $E_f = E(\text{Ti}_3\text{S}_3\text{Te}_2) - 3E(\text{Ti}) - 3E(\text{S}) - 2E(\text{Te})$, where $E(\text{Ti}_3\text{S}_3\text{Te}_2)$, $E(\text{Ti})$, $E(\text{S})$, $E(\text{Te})$ are the total energies of monolayer $\text{Ti}_3\text{S}_3\text{Te}_2$ per unit cell, single Ti, S, Te atoms in their bulk phase, respectively. The calculated E_f per unit cell of monolayer $\text{Ti}_3\text{S}_3\text{Te}_2$ is -0.24 eV, indicating an exothermic reaction during its formation. Additionally, an ab initio molecular dynamic (AIMD) simulation was performed to evaluate thermal stability of the monolayer at 300 K over a duration of 8 ps, as illustrated in Fig. S1(b). The slight fluctuations of total energy and geometry shows its thermal stability at room temperature.

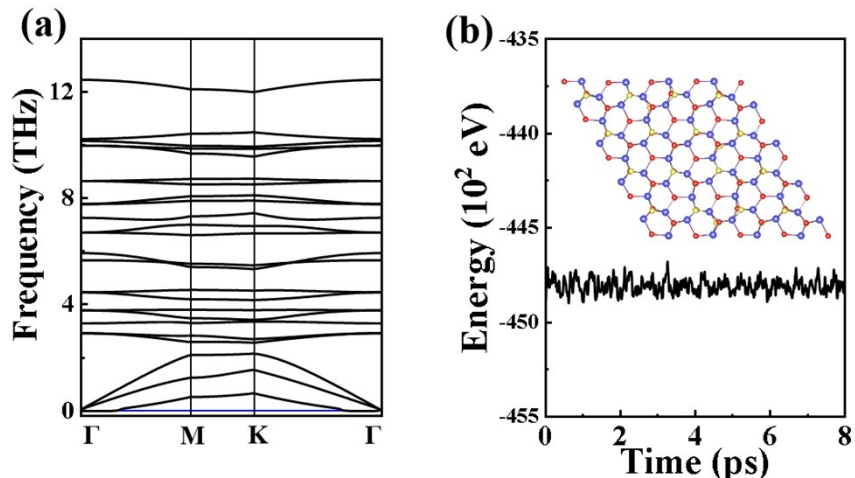


Fig. S1 (a) Phonon spectrum of monolayer $\text{Ti}_3\text{S}_3\text{Te}_2$. (b) The fluctuation of total energies of the monolayer $\text{Ti}_3\text{S}_3\text{Te}_2$ during ab initio molecular dynamic (AIMD) simulation at 300K, the inset in (b) shows the top view of $\text{Ti}_3\text{S}_3\text{Te}_2$ nanoflake after 8 ps simulation.

To explore the magnetic ground state, we considered one ferromagnetic (FM) and seven possible antiferromagnetic configurations, including two types of colinear ones (AFM1 and AFM2 [see Fig.S2]) and four types of noncolinear ones (AFM3, AFM4, AFM5 and AFM6 [see Fig.S2]) . The total energy difference of FM state and other AFM states are shown in Fig. S2, indicating a preference for the FM state in monolayer $\text{Ti}_3\text{S}_3\text{Te}_2$. To estimate the stability of the FM state, the Curie temperature (T_C) of the monolayer $\text{Ti}_3\text{S}_3\text{Te}_2$ was evaluated from Heisenberg model based on Monte

$$H = J_1 \sum_{\langle i,j \rangle} \mathbf{S}_i \cdot \mathbf{S}_j + J_2 \sum_{\langle\langle i,j \rangle\rangle} \mathbf{S}_i \cdot \mathbf{S}_j$$

Carlo simulations.^{1, 2} The Hamiltonian can be written as, where J_1 and J_2 are the effective exchange coupling parameter of nearest neighbor (NN) and next nearest neighbor (NNN), respectively. As shown in Fig. S3(a), the T_C of the monolayer $\text{Ti}_3\text{S}_3\text{Te}_2$ is 150 K, which can be determined by observing the peak of specific heat as a function of temperature, along with the sudden decrease in magnetic moment. The magnetic anisotropic energy (MAE) for $\text{Ti}_3\text{S}_3\text{Te}_2$ across the entire space are depicted in Fig.S3 (b). This visualization demonstrates that the magnetic easy axis is situated within the xoy plane, with an MAE value of approximately 615 μeV per unit cell.

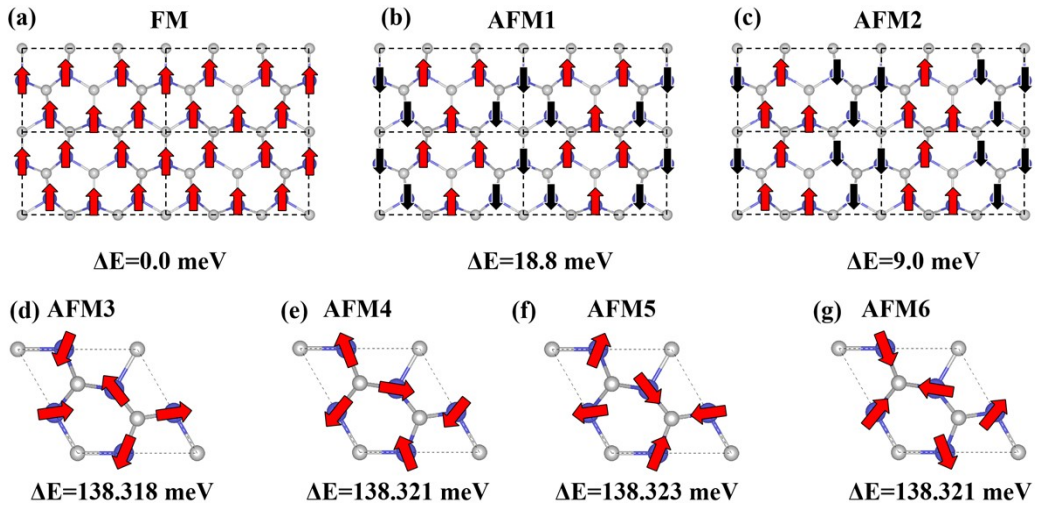


Fig. S2. Seven possible magnetic states of monolayer $\text{Ti}_3\text{S}_3\text{Te}_2$.

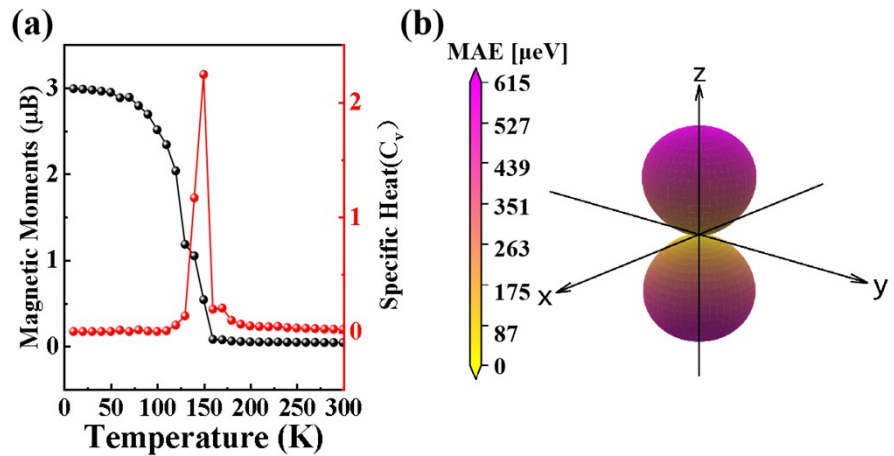


Fig. S3 (a) the magnetic moments and specific heat of monolayer $\text{Ti}_3\text{S}_3\text{Te}_2$ as a function of temperature. (b) The Angular dependence of magnetic anisotropy energy (MAE) of monolayer $\text{Ti}_3\text{S}_3\text{Te}_2$.

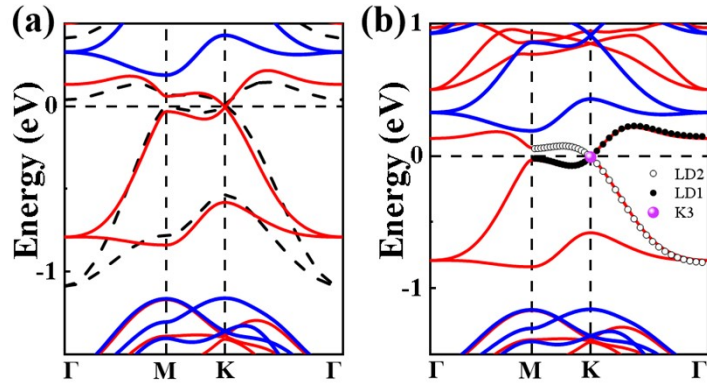


Fig. S4 The band structure of monolayer $\text{Ti}_3\text{S}_3\text{Te}_2$ without considering SOC effect. (a) Black dashed line represents the band structure obtain from TB model. (b) The white, black and light blue spheres donate the irreducible representation LD2, LD1, K3, respectively.

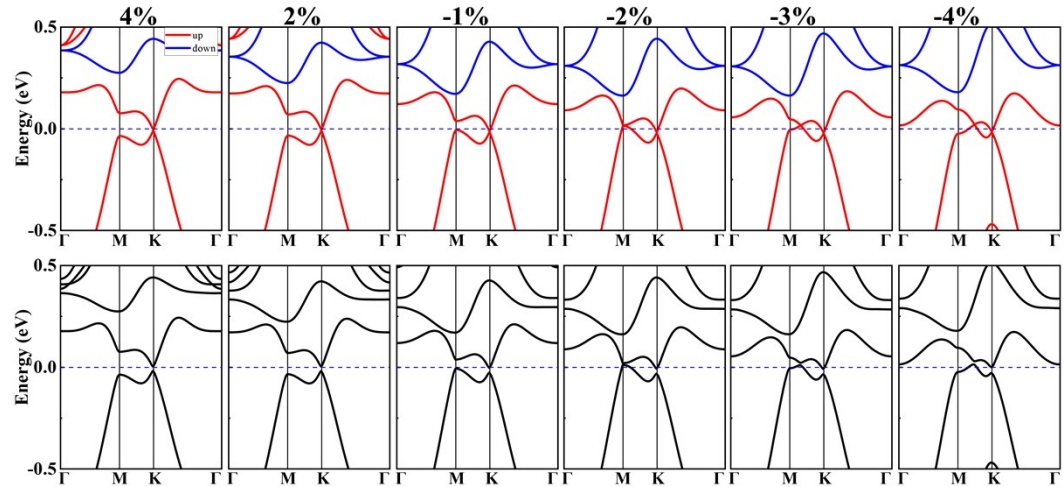


Fig. S5 Band structure of $\text{Ti}_3\text{S}_3\text{Te}_2$ monolayer without (with) SOC when the magnetization is along z direction and η is applied from -4% to 4%.

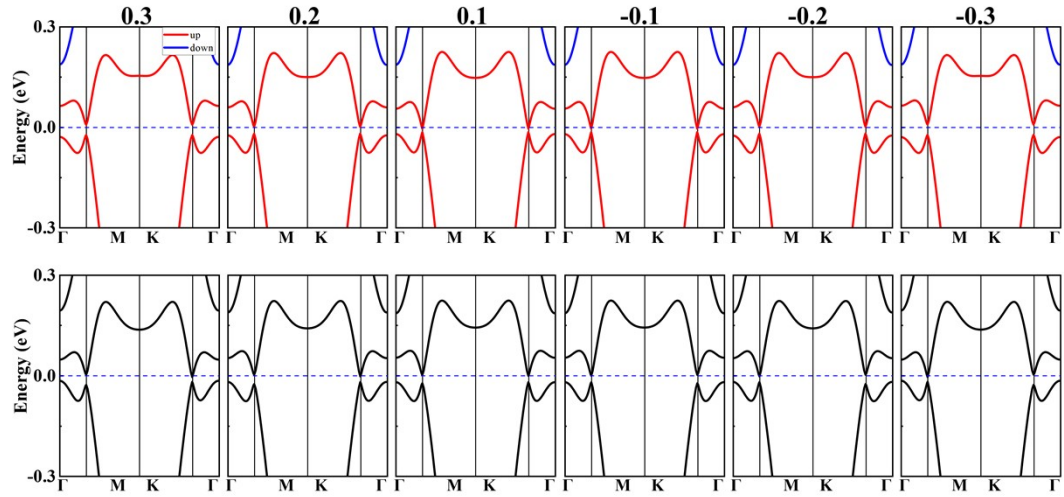


Fig. S6 Band structure of $\text{Ti}_3\text{S}_3\text{Te}_2$ monolayer without (with) SOC when the magnetization is along z direction and external electric fields is applied from 0.3 eV/Å to 0.3 eV/Å.

1 J. Zhang, Y. Shao, C. Li, J. Xu, H. Zhang, C. Wang, B. Wang and J. Cho, *Appl. Phys. Lett.*, 2024, **125**.

2 B. Wang, Y. Bai, C. Wang, S. Liu, S. Yao, Y. Jia and J. Cho, *Phys. Rev. B*, 2024, **110**, 094423.